

Crustal thickness beneath the Andes and Sierras Pampeanas at 30°S inferred from Pn apparent phase velocities

R. Fromm, G. Zandt, and S. L. Beck

Department of Geosciences, University of Arizona, Tucson, Arizona, USA

Received 5 December 2003; revised 2 February 2004; accepted 10 March 2004; published 31 March 2004.

[1] We obtained a 2D crustal model beneath central Chile and western Argentina using apparent Pn phase velocities recorded along an EW trending transect at 30°S. This model is characterized by a thick (65 km) crustal root beneath the High Cordillera, a 60 km thick crust beneath the Precordillera, and a gradual shallowing of Moho depths beneath the Sierras Pampeanas from 55 km in the west to 40 km in the east. Beneath the Sierras Pampeanas, where very little crustal shortening is observed, the thick crust must be explained by means other than simple tectonic shortening. Isostatically balanced crustal thickness is consistently shallower than our model shows, suggesting the existence of dynamic forces possibly linked to the flat slab. *INDEX TERMS*: 7203 Seismology: Body wave propagation; 7205 Seismology: Continental crust (1242); 9360 Information Related to Geographic Region: South America. **Citation**: Fromm, R., G. Zandt, and S. L. Beck (2004), Crustal thickness beneath the Andes and Sierras Pampeanas at 30°S inferred from Pn apparent phase velocities, *Geophys. Res. Lett.*, *31*, L06625, doi:10.1029/2003GL019231.

1. Introduction

[2] The tectonic evolution of the south-central Andes in central Chile and western Argentina at around 30°S is the result of a complex interaction between the South American plate and the segment of the Nazca Plate that carries the Juan Fernandez Ridge. The orogenic system as a whole started to form much earlier, but major present day regional structures acquired their present configuration predominantly since the Miocene [Ramos *et al.*, 2002]. Volcanic arc activity between 29°–30.5° coincided with the High Cordillera until ~11 Ma ago, after which magmatism migrated over 500 km eastward shutting off completely around 5 Ma. This is consistent with a coeval gradual shallowing of the subducting slab [Kay *et al.*, 1988]. Overall, 150–170 km of crustal shortening in the upper crust has been documented to be accommodated almost exclusively by thin-skinned fold and thrust belts in the High Cordillera and Precordillera [Allmendinger *et al.*, 1990]. Further east, thick-skinned basement cored uplift in the 400 km wide Sierras Pampeanas was possibly triggered by the flattening of the slab during the last 5–7 Ma [Ramos *et al.*, 2002]. A causal dependence of the flattening of the slab and the subduction of the Juan Fernandez Ridge at these latitudes around 12 Ma ago has been proposed by several authors [Gutscher *et al.*, 2000; Yañez *et al.*, 2002]. Moreover, the colder mantle wedge associated with the

thermal shielding of the flat slab might dynamically link the subducting and overriding plates [Gutscher *et al.*, 2000].

[3] In this context, the shape of the Moho and the absolute crustal thickness provide important constraints on the tectonic evolution of the region. Allmendinger *et al.* [1990] used balanced cross sections to estimate crustal thickening caused by crustal shortening and proposed a model with maximum Moho depths of ~60 km beneath the High Cordillera. Regnier *et al.* [1994] used local slab events to record S to P converted phases at the Moho, obtaining similar maximum crustal thicknesses near the Sierra Pie de Palo located about 100 km south of the Bermejo Valley. Recent modeling of gravimetric data in the Bermejo basin suggests a maximum crustal thickness of 45–60 km [Gimenez *et al.*, 2000]. Surface mapping in combination with some limited deep seismic reflection data indicates the presence of mid crustal fault systems [Allmendinger *et al.*, 1990; Ramos *et al.*, 2002], which show a possible connection between shallow and deep deformation. However, the detailed mechanisms that relate shallow crustal deformation to deep crustal thickening in the Sierras Pampeanas are still poorly understood. In this paper, we use apparent Pn phase velocities to construct a 2D crustal model in the vicinity of 30°S, thereby constraining the crustal thickness in this tectonically complex region.

2. Data and Methodology

[4] As part of the CHile ARgentina Geophysical Experiment (CHARGE), 8 broadband stations were deployed in central Chile and Argentina along a west-to east-trending transect around 30°S, recording continuous data from November 2000 to May 2002 (Figure 1a). Seismic waves generated by off-shore crustal earthquakes west of the profile were recorded at distances ranging from 100–700 km. For this distance range, the first arrival generally corresponds to the head wave traveling along the Moho discontinuity (Pn waves). In total, 9 crustal events were large enough for the first arrival to be picked on most of the stations (Figure 1a). Unfortunately, no crustal events of sufficient magnitude east of the profile could be identified to record rays traveling in the reverse direction.

[5] Baumont *et al.* [2001] successfully determined crustal thicknesses beneath the Bolivian Altiplano using absolute Pn travel times of one event recorded at a dense station profile. However, the much lower station density available for this study imposes the need to use several events, which makes it difficult to use absolute travel times due to uncertainties in the hypocenter locations and near source structural complexities. Therefore, apparent phase velocities, defined as the ratio between the travel time and

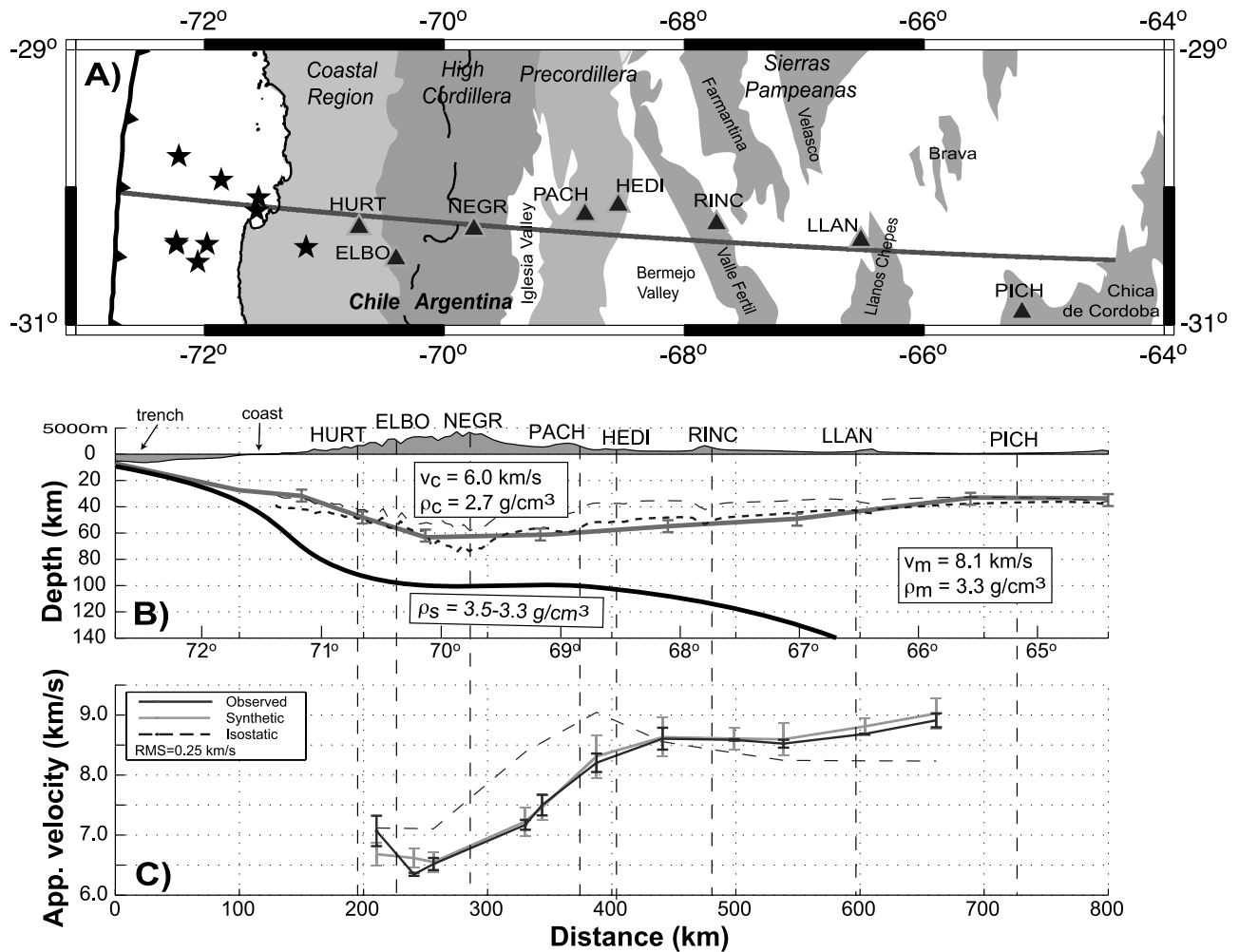


Figure 1. A) Map showing the region of study. Major geological units are modified from [Allmendinger *et al.*, 1990] and [Ramos *et al.*, 2002]. The seismic stations are plotted as triangles, the events as stars and the profile corresponds to the thick gray line. B) Cross section showing the Moho (thick gray line) and the slab (thick black line) given by [Cahill and Isacks, 1992]. Dashed lines correspond to isostatic crustal thicknesses without (long dashed) and with (short dashed) lateral density variations in the slab. P-wave velocities and densities of the crust, mantle and slab are given in the boxes. C) Apparent interstation phase velocities along the profile defined in A). Black line corresponds to observed phase velocities, gray line to synthetic values given by our preferred model in B) and the dashed line to the isostatic crustal model without the slab (long dashed line in B).

horizontal distance, will be used to partially overcome these problems. For two stations aligned along a single profile, the differential or interstation apparent phase velocity c is defined as

$$c = \frac{\Delta x}{\Delta t} = \frac{x_{i+1} - x_i}{t_{i+1} - t_i} \quad (1)$$

where t and x are the travel times and epicentral distances at two consecutive stations i and $i + 1$, respectively, along the profile. Because Pn waves share a similar travel path until the point where the ray re-emerges into the crust, c is independent (at least to first order) of errors in the hypocentral location, origin times and velocity structure close to the source. Moreover, variations in c along the profile primarily reflect changes of crustal thickness (and therefore the dipping of the Moho) and changes of velocities in the crust and underlying mantle. Because the actual

observed apparent phase velocity will represent an integrated effect along the ray path, the observations are arbitrarily but conveniently considered to be representative of the midpoint between the two consecutive stations. For modeling purposes, lateral crustal heterogeneity along the profile is ignored, thereby limiting the variations to changes in crustal thickness. Using multiple events, more than one phase velocity observation can be computed for each station pair or midpoint. The average crustal phase velocity and standard deviation are computed for each midpoint for all the observations. It can be shown that for a profile along which the Moho interface has a change of its dip, the apparent phase velocities are dependent on the absolute thickness of the crust. The reason for this is that the time each crustal ray leg spends in the crust depends on the angle of dip of the Moho at the point the ray reenters the crust. As long as the dip of the interface changes along the profile, each crustal ray samples the crust at different angles making

Table 1. Inversion Parameters

Parameter	Stage 1	Stage 2
	Models 1–1000	Models 1001–2000
Crustal velocity	5.8–6.5 km/s	5.8–6.3 km/s
Mantle velocity	7.8–8.5 km/s	7.8–8.3 km/s
Moho depths	±15 km	±5 km

the phase velocities sensitive to absolute crustal thicknesses. This was confirmed by the sensitivity analysis presented below.

[6] Our next step is to find a crustal model which best fits the observed apparent phase velocities. The forward model is solved using the 2D ray tracer RayInvr [Zelt and Forsyth, 1994], which can explicitly account for head waves and arbitrary interface geometries. To restrict the number of unknown parameters, we assume homogeneous crustal (v_c) and mantle (v_m) velocities, and local Moho depths at 8 points along the profile, defining a total of 10 free parameters. The first stage of the inversion consists of using a trial and error approach to find a velocity structure that approximates the observed phase velocities along the profile. Phase velocities were computed for each midpoint using equation (1), and averaged for all the events. The misfit is defined as the RMS value between observed and calculated apparent phase velocities. To avoid any bias caused by our choice of the initial model, we use our preliminary model as a reference and compute 2000 randomly perturbed models and compare them to the observations. We chose as the best model the one with the smallest RMS value. To refine the search interval in model space, the random search was split into two stages. Table 1 lists the intervals the parameters were allowed to vary for each stage. After the first 1000 models, the best model was chosen as a new reference and another 1000 models were tested.

3. Results

[7] Observed apparent phase velocities (Figure 1c) are relatively small beneath the High Cordillera (~6.0–7.0 km/s), and increase towards the east under the Precordillera (~8.0 km/s). Further east, under the Sierras Pampeanas, apparent phase velocities gradually increase, reaching a maximum velocity of 8.5 km/s between stations LLAN and PICH. This velocity structure indicates a thick crustal root beneath the high Andes and a westward dipping Moho under the Precordillera and Sierras Pampeanas. Our preferred model obtained with the inversion outlined in the previous section is shown in Figure 1b. The crust reaches a maximum thickness of 65 km under the High Cordillera and gradually decreases towards the east, where a crustal thickness of 36 km is indicated beneath station PICH. This crustal model coincides well with a converter obtained by receiver function analysis along the profile [Gilbert *et al.*, 2003].

4. Sensitivity Analysis

[8] It is important to address the uniqueness and robustness of this solution. To assess the sensitivity and tradeoffs between different parameters, the subset of the model space defined in stage 2 (Table 1) was discretized and the RMS values were plotted for different combinations of crustal/mantle velocities and maximum crustal thicknesses

(Figure 2). The best model with the lowest misfit was found to have a mantle velocity $v_m = 8.10$ km/s, crustal velocity $v_c = 6.0$ km/s, and a maximum crustal thickness of 60–65 km. Considering the broad minimum of the misfit surface (right column in Figure 2), crustal velocity and maximum thickness are only weakly constrained. Maximum thickness variation measures the vertical offset of the whole profile. The absolute thicknesses for any other point along the profile could have been used equivalently.

[9] To estimate the uniqueness of the solution, uncertainties of the model parameters were mapped into phase velocity space, by computing 2000 synthetic apparent phase velocity profiles. We allowed random perturbations of our preferred model of ± 0.2 km/s in crustal velocity, ± 0.1 km/s in mantle velocity and ± 5 km in Moho depth. With this set of synthetic phase velocities, a distribution of theoretical apparent phase velocities for each mid-point along the profile can be constructed and the interval containing 66% of the samples determined. This interval (corresponding to the synthetic error bars in Figure 1b) are compared to the standard deviation of the observations. In general, a good fit between the synthetic and observed phase velocities and their respective errors can be observed.

5. Isostatic Crustal Thickness

[10] We compare our seismically obtained crustal model to an isostatically compensated crustal thickness model.

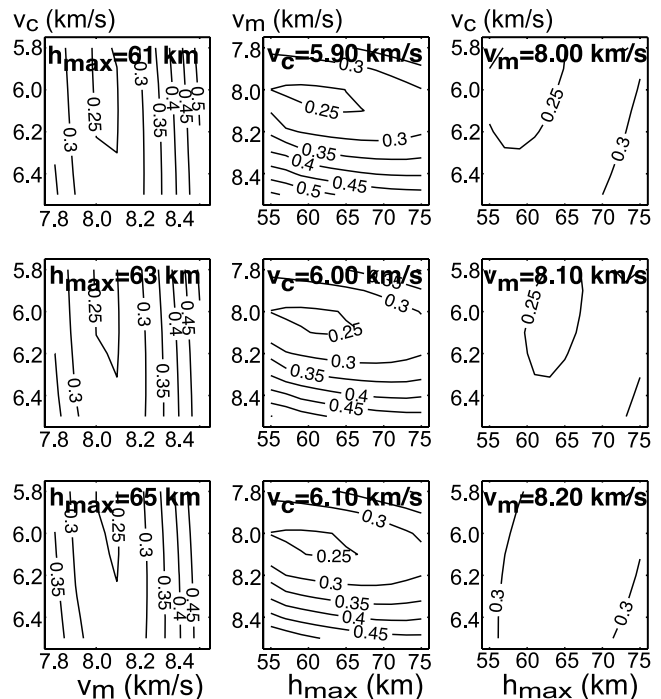


Figure 2. Trade-off of crustal velocity (v_c), mantle velocity (v_m) and maximum crustal thickness (h_{max}) over the RMS misfit. The first column shows the relation between crustal and mantle velocity for different thicknesses, the second column shows the trade-off between mantle velocity and reference thickness for different crustal velocities, and the third column shows the trade-off between crustal velocity and reference thickness for different mantle velocities.

This model consists of Moho depths computed as a function of topographic elevations, where local isostatic compensation without flexural support is assumed and a range of realistic crustal, mantle and slab densities were tested. The reference model was assumed to be beneath station PICH (crustal thickness of 36 km). The resulting crustal thickness dictated by isostasy is consistently thinner (up to 20 km) than our model beneath the Precordillera and western Sierras Pampeanas. We could match the isostatic and seismically determined crust by considering a heavier slab with a laterally varying average density corresponding to 3.5 g/cm^3 beneath the high Cordillera in the flat segment of the slab and 3.3 g/cm^3 beneath the eastern Sierras Pampeanas where the slab resumes its normal dip (Figure 1a). However, these densities are generally too high for a buoyant flat slab to exist [van Hunen *et al.*, 2002] and are inconsistent with the expected basalt to eclogite transition in the oceanic crust as the plate subducts towards the east [Hacker, 1996]. A similar test shows that a heavier crustal model with average densities of over 2.9 g/cm^3 in the western Sierras Pampeanas and 2.7 g/cm^3 elsewhere could compensate the observed mass deficit. Gimenez *et al.* [2000] obtained similar crustal thicknesses modeling the regional Bouguer anomaly in the Bermejo basin in the westernmost Sierras Pampeanas (Figure 1a). However, their average density of 2.77 g/cm^3 is too low compared to the more than 2.9 g/cm^3 required to explain the observed mass deficit. Finally, considering a heterogeneous mantle wedge ($\sim 35\text{--}45 \text{ km}$) requires unrealistically large density variations, rendering the mantle as an unlikely source to explain the observed anomaly.

6. Discussion and Conclusions

[11] Using apparent Pn phase velocities to determine crustal thicknesses is shown to be a reliable method. The method allows the estimation of uncertainties and tradeoffs between different parameters of the model. The computed P-wave average crustal velocity of 6.0 km/s is relatively slow compared to the global average, but is consistent with other observations in the central Andes [e.g., Swenson *et al.*, 2000]. Besides, higher velocities would require even larger crustal thicknesses to explain the same observed anomalies.

[12] A maximum crustal thickness of 65 km beneath the High Cordillera and $\sim 60 \text{ km}$ in the Precordillera is consistent with a crustal model obtained by balanced cross sections [Allmendinger *et al.*, 1990]. Further east, where only minor crustal shortening has been observed in the Sierras Pampeanas, the abnormally thick crust of $45\text{--}55 \text{ km}$ that we measured must be explained by other processes.

[13] The observed discrepancy between the seismically determined Moho depths and an isostatically compensated model might be explained by a specific combination of crustal, mantle and slab densities. However, since we do not have good constraints on lateral density variations on a

regional scale, we tested a suit of simple density distributions in the crust, mantle and slab. As discussed above, these heavier density profiles are an unlikely source since the required density anomalies are unrealistic or inconsistent with expected values. Consequently, it may be necessary to explain the low elevations associated with the anomalously thick crust in the western Sierras Pampeanas by dynamic effects related to the subducting flat slab.

[14] **Acknowledgments.** This work was supported by NSF grant EAR9811870. Seismic data was acquired at seismic stations provided by the IRIS/PASSCAL program. We thank Hersh Gilbert for his helpful discussions and two anonymous reviewers for their critical comments and the encouraging skepticism of Arda Ozacar.

References

- Allmendinger, R. W., D. Figueroa, D. Snyder, J. Beer, C. Mpodozis, and B. L. Isacks (1990), Foreland shortening and crustal balancing in the Andes at 30°S latitude, *Tectonics*, *9*, 789–809.
- Baumont, D., A. Paul, G. Zandt, and S. L. Beck (2001), Inversion of Pn travel times for lateral variations of Moho geometry beneath the central Andes and comparison with the receiver functions, *Geophys. Res. Lett.*, *28*, 1663–1666.
- Cahill, T. A., and B. L. Isacks (1992), Seismicity and shape of the subducted Nazca Plate, *J. Geophys. Res.*, *97*, 17,503–17,529.
- Gilbert, H., S. L. Beck, G. Zandt, and CHARGE Working Group (2003), Crustal structure of central Chile and Argentina, *Eos Trans. AGU*, *84*(46), Fall Meet. Suppl., S41F-05.
- Gimenez, M. E., M. P. Martinez, and A. Introcaso (2000), A crustal model based mainly on gravity data in the area between the Bermejo Basin and the Sierras de Valle Fertil, Argentina, *J. S. Am. Earth Sci.*, *13*, 275–286.
- Gutscher, M. A., W. Spakman, H. Bijwaard, and E. R. Engdahl (2000), Geodynamics of flat subduction: Seismicity and tomographic constraints from the Andean margin, *Tectonics*, *19*, 814–833.
- Hacker, B. R. (1996), Eclogite formation and the rheology, buoyancy, seismicity, and H_2O content of oceanic crust, in *Subduction: Top to Bottom*, *Geophys. Monogr. Ser.*, vol. 96, edited by G. E. Bebout *et al.*, pp. 337–346, AGU, Washington, D. C.
- Kay, S. M., V. Maksaev, R. Moscoso, C. Mpodozis, C. Nasi, and C. E. Gordillo (1988), Tertiary Andean magmatism in Chile and Argentina between 28°S and 33°S : Correlation of magmatic chemistry with a changing Benioff zone, *J. S. Am. Earth Sci.*, *1*, 21–38.
- Ramos, V. A., E. O. Cristallini, and D. J. Pérez (2002), The Pampean flat-slab of the central Andes, *J. S. Am. Earth Sci.*, *15*, 59–78.
- Regnier, M., J. M. Chiu, R. Smalley, B. L. Isacks, and M. Araujo (1994), Crustal thickness variation in the Andean foreland, Argentina, from converted waves, *Bull. Seismol. Soc. Am.*, *84*, 1097–1111.
- Swenson, J. L., S. L. Beck, and G. Zandt (2000), Crustal structure of the Altiplano from broadband regional waveform modeling: Implications for the composition of thick continental crust, *J. Geophys. Res.*, *105*, 607–621.
- van Hunen, J., A. P. van den Berg, and N. J. Vlaar (2002), On the role of subducting oceanic plateaus in the development of shallow flat subduction, *Tectonophysics*, *352*, 317–333.
- Yañez, G., J. Cembrano, M. Pardo, C. R. Ranero, and D. Selles (2002), The Challenger-Juan Fernandez-Maipó major tectonic transition of the Nazca-Andean subduction system at $33^\circ\text{--}33^\circ\text{S}$: Geodynamic evidence and implications, *J. S. Am. Earth Sci.*, *15*, 23–38.
- Zelt, C. A., and D. A. Forsyth (1994), Modeling wide-angle seismic data for crustal structure: Southeastern Grenville Province, *J. Geophys. Res.*, *99*, 11,687–11,704.

G. Zandt, S. L. Beck, and R. Fromm, Department of Geosciences, University of Arizona, Gould-Simpon Building, 1040E Fourth St., Tucson, AZ 85721, USA. (rfr@geo.arizona.edu)